AD-A274 152

▌▌▌▌▌▌▌▌▌▌▌▌▌▌▌

copy no.

title

TNO-report
FEL-93-B047

Light Emitting Porous Silicon

DTIC
ELECTE
DEC 2 7 1993
A

author(s):

H.H.P.Th. Bekman, K.W. Benoist,

J.L. Joppe, H.J. van Weerden

date:

May 1993

classification

title	: ongerubriceerd
abstract	: ongerubriceerd
report text	: ongerubriceerd

no. of copies	: 25
no. of pages	: 30 (excluding RDP and distribution list)
no. of appendices	: -

All information which is classified according to Dutch regulations shall be treated by the recipient in the same way as classified information of corresponding value in his own country. No part of this information will be disclosed to any party.

The classification designation ongerubriceerd is equivalent to unclassified.

93-31044

93 12 22 1 57

Best Available Copy

report no.	:	FEL-93-B047
title	:	Light Emitting Porous Silicon
author(s)	:	Dr. H.H.P.Th. Bekman, K.W. Benoist, J.L. Joppe, and H.J. van Weerden
institute	:	TNO Physics and Electronics Laboratory
date	:	May 1993
NDRO no.	:	-
no. in pow '92	:	715.4
Research supervised by :		J.L. Joppe
Research carried out by :		Dr. H.H.P.Th. Bekman, K.W. Benoist, J.L. Joppe, and H.J. van Weerden

ABSTRACT (ONGERUBRICEERD)

After a review of the basic properties of porous silicon we describe the fabrication method we employed to produce visible light emission from silicon. The photo-luminescence spectra were recorded using a room-temperature spectrometer. Initial attempts producing electrically stimulated light emission are described. Two pressure experiments were carried out to unravel the origin of light emission in porous silicon.

rapport no.	:	FEL-93-B047
titel	:	Licht emitterend poreus silicium
auteur(s)	:	Dr. H.H.P.Th. Bekman, Drs. K.W. Benoist, Drs. J.L. Joppe, en H.J. van Weerden
instituut	:	Fysisch en Elektronisch Laboratorium TNO
datum	:	mei 1993
do-opdr.no.	:	-
no. in lwp '92	:	715.4
Onderzoek uitgevoerd o.l.v.	:	Drs. J.L. Joppe
Onderzoek uitgevoerd door	:	Dr. H.H.P.Th. Bekman, Drs. K.W. Benoist, Drs. J.L. Joppe, en H.J. van Weerden

SAMENVATTING (ONGERUBRICEERD)

Nadat een overzicht is gegeven van de belangrijkste eigenschappen van poreus silicium wordt onze fabricage van licht emitterend silicium beschreven. De fotoluminescentie spectra werden opgenomen met een op kamertemperatuur werkende spectrometer. Eerste pogingen om te komen tot elektrisch gestimuleerde licht emissie worden beschreven. Twee druk experimenten zijn uitgevoerd om de oorsprong van de licht emissie in poreus silicium te achterhalen.

1 INTRODUCTION

Silicon is the second most abundant element in the earth's crust. In its crystalline form it is extremely well characterized and studied. Big monocrystalline silicon crystals of extreme purity can nowadays be produced without difficulty. It has become the basic building block of the electronics industry, and it is unlikely to be replaced for a long time. Despite its superiority silicon is not exclusively used in the semiconductor industry. High frequency integrated circuits are best made in gallium-arsenide (GaAs) a III-V semiconductor, because of its larger electron mobility. Another severe drawback is silicons inability to efficiently generate light. Typically only one photon is created for 10^4-10^5 electrically injected carriers, due to the indirect nature of the bandgap. The emission wavelength is in the infrared (1.09 eV). Instead, more complex, compound semiconductor materials, based on GaAs, and InP are used. They possess direct bandgaps, and consequently efficient light generation. The development of a silicon-based optoelectronic material that would allow optical devices such as lasers and light-emitting diodes to be easily integrated with electronic components (OEIC's) has been a long-standing goal of the materials physics community.

One way to raise the radiation efficiency of silicon is to introduce impurity-activated optical transitions. For radiative recombinations to dominate the nonradiative channels, the optically active impurity must be present at relatively high concentrations. Rare-earth dopants (Erbium, Ytterbium) are possible candidates. Erbium has internal transitions around 1.54 μm, which is favourable for low-loss optical fibre communication, and is successfully applied in fibre amplifiers [1]. When erbium is introduced into silicon at the required high concentration segregation occurs [2]. Another attempt makes use of a carbon related defect [3].

In 1990 Canham discovered that so-called 'porous silicon' emits rather intense visible light following optical excitation [4]. Depending on the preparation conditions the emission wavelength can be varied from IR to green with external quantum efficiencies of a few percent. Because of its potential applications the discovery by Canham initiated a world-wide research effort. The key questions to be answered: Why does porous silicon efficiently emit visible light? Can it be used in practical applications? In this paper we hope to shed some light on these matters.

2   PREPARATION

Porous silicon layers can be formed in two different ways. In the first silicon wafers are etched in solutions of $HF:HNO_3:H_2O$ with ratios of 1:5:10 or 4:1:5 (by volume) [5]. In the second, as originally used by Canham, a silicon sample is anodically etched in aqueous hydrofluoric acid. Figure 1 shows the typical I-V characteristics for n- and p-type silicon.

(a)

(b)
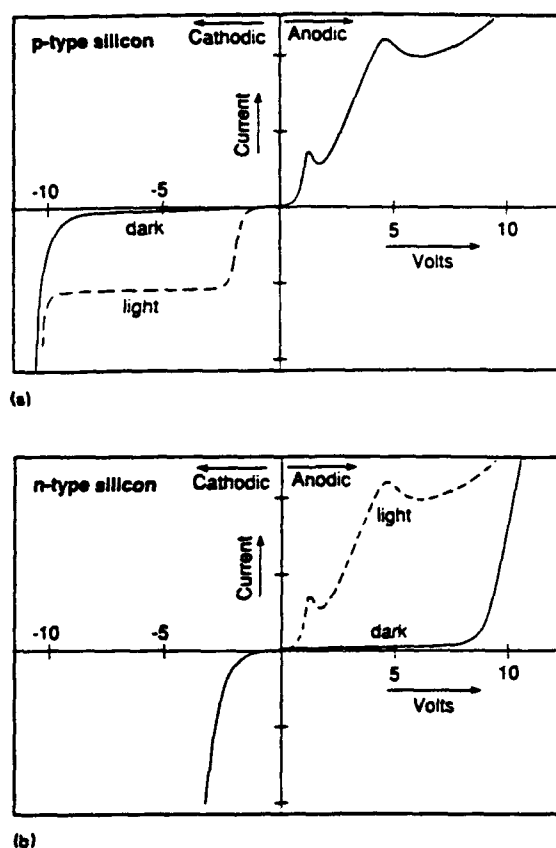
Fig.1.   Typical current-voltage relationships for n- and p-type silicon. Above the first current peak electro-polishing starts [6].

Under cathodic polarizations for both n- and p-type material silicon is normally stable. Only under anodic polarizations silicon dissolution occurs. However depending upon the magnitude of the anodic potential, drastically different surface morphologies result [7]. At high anodic overpotentials, the silicon surface electropolishes and the surface retains a relatively smooth and planar morphology. In direct contrast at low anodic overpotentials the surface morphology is

dominated by a vast labyrinth of channels that can penetrate deep into the bulk of the silicon. Size, shape, thickness and density depend on exact anodisation conditions i.e. HF concentration, temperature, silicon dopant and concentration, anodisation time, illumination etc.

The exact dissolution chemistries of silicon are still in question, although it is generally accepted that holes are required in the initial oxidation steps for both electropolishing and pore formation. This means that for n-type material significant dissolution occurs only under illumination, high fields or other hole generation mechanisms. During pore formation hydrogen gas evolves which disappears during electropolishing. The dissolution reaction as proposed by Lehmann and Gösele [8] is shown in Fig.2 .
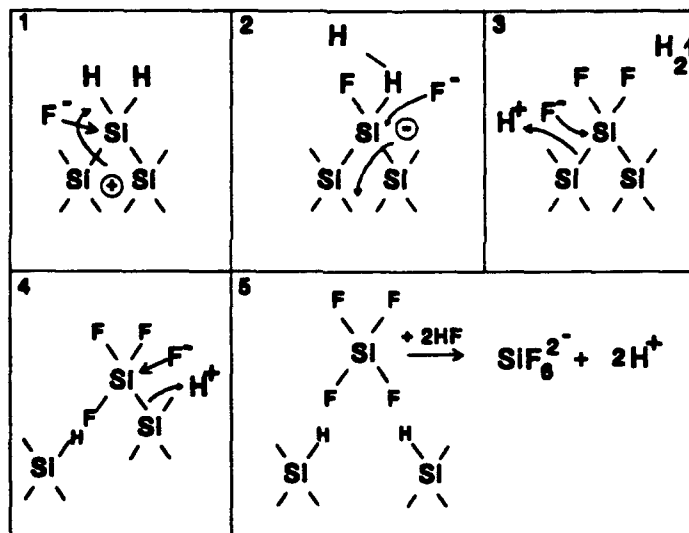
Fig.2.   Proposed dissolution mechanism of silicon electrodes in hydro-fluoric acid.

Inner surfaces of freshly prepared porous silicon layers (PSL) were found to be covered with hydrogen [9]. A silicon surface saturated with hydrogen is virtually inert against further attack of fluoride ions in an hydrogen fluoride (HF) solution. Under carrier injection however Si-H bonds can be replaced by Si-F bonds upon arrival of a hole (h^+) on the surface. This eventually lead to dissolution of the silicon atom.

If a silicon atom is removed from an atomically flat surface by the above reaction an atomic size dip remains. This change in surface geometry will change the dissolution mechanism in such a way that it preferentially occurs at the atomic dip. So surface inhomogeneities are amplified. The mechanism behind this pore formation is also part of a scientific discussion. Presently there are

three separate models which account for pore formation. In the Beale model [10-12] it is suggested that the interpore regions have reduced mobile carrier concentration due to overlapping depletion regions. Current is then selectively directed to the pore tips as a result of the high-resistance depleted porous structure. In another model Smith and co-workers [6,13] explain pore formation resulting from a stoichastic random walk of carriers to the silicon surface. The nature of the random walk presents the pore tips as the most likely contact site for a particle diffusing from the bulk of the semiconductor. In the third model by Lehmann and Gösele [8] quantum confinement in the interpore regions widens the bandgap locally. The resulting potential step induces a depletion region inside the unattacked surface region which protect it from further dissolution, and is in that respect similar to the Beale model.

Porous silicon morphologies are usually grouped into four basis groups n, p, n+, p+. For p-type silicon both the pore diameters and interpore spacing are extremely small, generally between 1 and 5 nm with a highly interconnected and homogeneous pore network. As the dopant concentration increases, the pore diameters and interpore spacing also increase slightly. For n-type the pore diameter and average interpore spacing decrease with increasing dopant concentration. The pore diameters in n-type silicon are considerably larger than in p-type silicon and show a strong tendency to form straight channels at low dopant concentrations rather than the randomly directed pore network of p-type silicon. The pore morphologies and diameters of p+ and n+ porous silicon are comparable, they tend to form small 5-10 nm channels with numerous side branches. For both p- and n-type pore propagation occurs in <100> directions [14,15]. Pore formation can be explained by the models mentioned in the previous paragraph. E.g. in the diffusion model by Smith et al. [6,13] the diffusion length of the holes, which is a function of the dopant concentration, voltage, etc., controls the different pore morphologies.

3   ORIGIN OF LIGHT EMISSION

The origin of visible luminescence in porous silicon (PS) is still controversial. A vigorous debate is going on. PS can emit light with peak energies in the range 1.12 eV (infra-red) to about 2.3 eV (green). The origin of light emission was originally explained by Canham by invoking size dependent quantum confinement effects [4]. Other possible explanations for the unusual properties of luminescent PS have in the mean time appeared. These generally rely on structural or compositional changes occurring during the electrochemical etch process.

3.1   Quantum confinement

It has been known for about a decade that the bandgap of isolated semiconductor crystallites, of strongly luminescent materials such as CdSe, increases in energy as diameter decreases in the 5 nm range. This occurs because the electron and hole acquire in small crystallites a significant quantum energy of localisation which increases the recombination energy. Figure 3 shows the photo-luminescence (PL) as function of crystallite size.
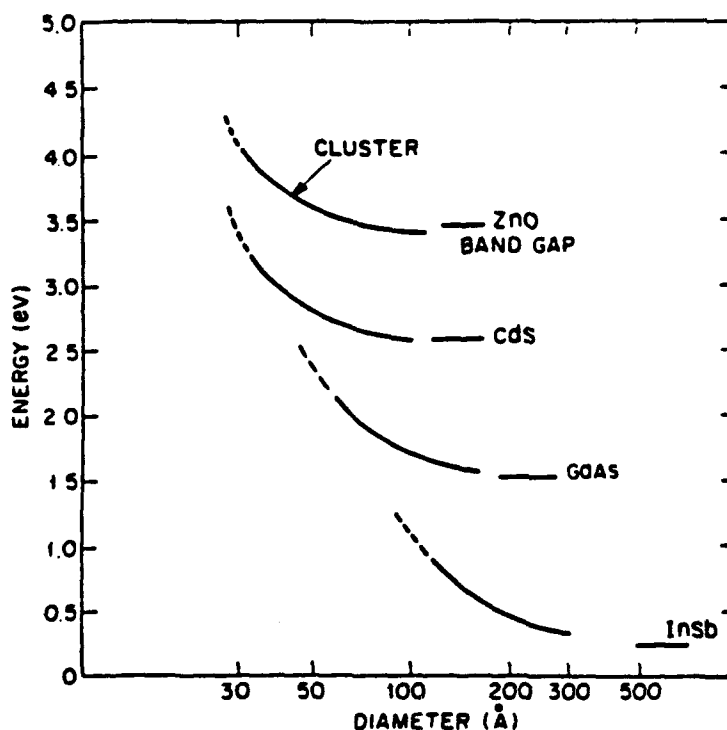

Fig.3.   Calculated dependence of crystallite band gap (left) on diameter and the bulk gap (right) for several semiconductors after L. Brus [16].

Silicon is different in that bulk luminescence is forbidden by selection rules due to its indirect bandgap. A breakdown of these rules has been confirmed by a group at Canon Research Centre who discovered that isolated 3-5 nm Si crystallites in glass emit visible light similar to that of PS [17]. They attributed their observations to quantum confinement. Decreasing the size of a crystal in all directions will confine the electrons and holes in real space with corresponding spread of the wavefunction in momentum space. Eventually if the size is sufficiently decreased the term indirect semiconductor is a misnomer.

Canham originally proposed that the quantum size effect in PS is related to the diameter of the silicon wire-like structures [4]. Electron microscopy suggest that PS of low porosity can be adequately approximated by bulk material containing an array of non interacting cylindrical pores of fixed radius that run perpendicular to the surface [10]. An anodized (100) face of a layer of relatively low porosity (25%) is shown in Fig.4a. In reality, of course, there is pore branching and variations in pore size separation, and perhaps even pore shape. Figures 4b, and 4c show the effect of subsequently increasing the porosity of the layer with an etchant that enlarges each pore by chemical dissolution. For cylindrical pores, porosities greater than 78.5% promote substantial merging of nearest-neighbour pores and consequently the physical isolation of a significant density of silicon columns.

(a) 25% POROSITY HOLE

(b) 50% POROSITY

(c) 80% POROSITY SILICON
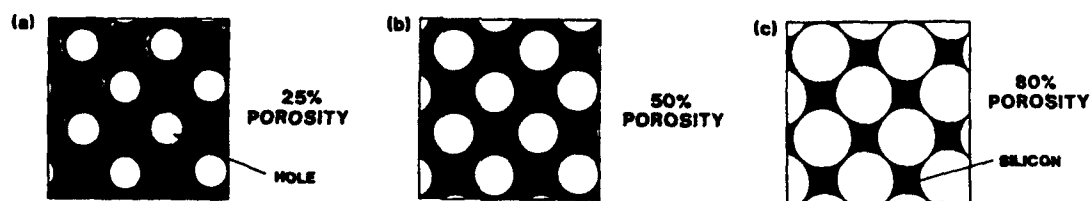
Fig.4.   Idealized plan view of an anodized (100) silicon wafer containing cylindrical holes. The indicated changes in porosity are achieved by pore enlargement through chemical dissolution, after Canham [4].

A rough estimate of the confinement energies in porous crystalline silicon needles can be obtained as follows. Let z be the <001> direction, L the transverse dimensions of the needles in the x and y directions, and assume that the carriers are confined in infinitely deep potentials. With needles pointing along the <001> direction, there exist two kinds of confinement for electrons. They respectively arise from (1) the two conduction ellipsoids with their axis of revolution lined

up with the needle and (2) the four other conduction ellipsoids which point along the <100> and <010> directions. Note that these four ellipsoids give rise to degenerate confinement energies because of the assumption of equal wire thickness along the x and y directions. If m_t and m_l are the transverse and longitudinal effective masses in silicon near the Δ point (0.2 m_o and m_o respectively) we obtain the conduction band edge energies due to confinement equal to:

$$E^{(1)} = \frac{\hbar^2 \pi^2}{m_t L^2} \tag{1}$$

$$E^{(2)} = \left(1 + \frac{m_t}{m_l}\right) \frac{\hbar^2 \pi^2}{2 m_t L^2} \tag{2}$$

This is to be compared with a 1-dimensional particle in a box problem which has solutions of:

$$E_n = \frac{\hbar^2}{2m} \left(\frac{n\pi}{L}\right)^2 \qquad n = 1,2,3... \tag{3}$$

In addition the hole confinement energy has to be taken into account. No analytic expression is available. For a wire of 3 x 3 nm one can calculate the electron confinement to be 252 meV (Eq. 2) and the hole confinement 371 meV which makes 620 meV all together [18]. For silicon wires of 3 x 3 nm the model predicts luminescence at 721 nm wavelength (1.1 + 0.62 = 1.72 eV, red-orange).

One of the strongest evidences for the confinement model is the observation that increased etching in HF solutions (so after the anodic etching step) results in higher energy luminescence presumably caused by a reduction in feature size (see Fig.5).
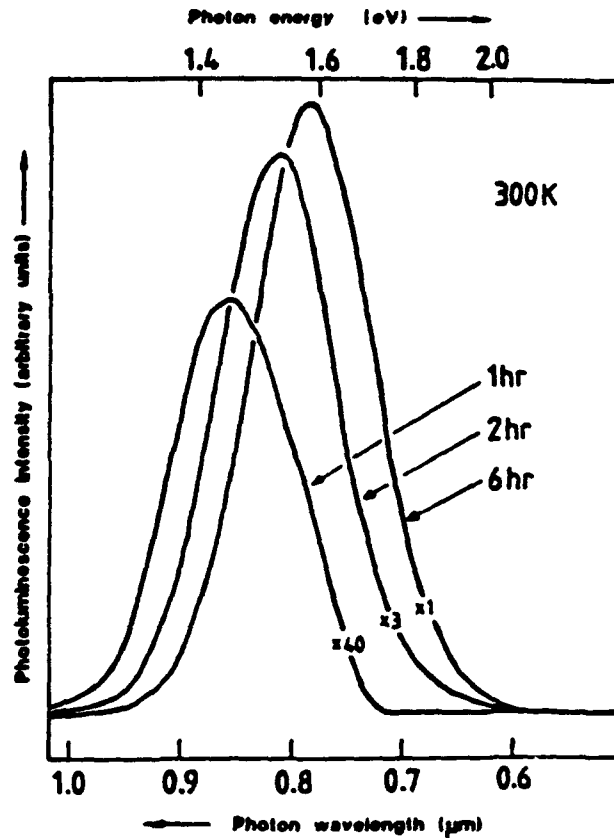
Fig.5.   Room-temperature photoluminescence from anodized p-type wafer after immersion in 40% aqueous HF for the times indicated [4].

3.2   Siloxene

Another proposed explanation for PS luminescence proposes that the electrochemical etch generates a surface or bulk chemical species. Siloxene, a chemical which contains silicon oxygen and hydrogen has emissive properties that are very similar to those of PS. Stutzmann et al. [19] demonstrated similarities in the chemical luminescence, photoluminescence, infra-red, Raman, and excitation spectra, as well as the emission lifetimes and chemical fatigue behaviour for the two materials. This data makes a strong case for the presence of a siloxene or similar species in porous silicon. However, one difference between the chemical siloxene and luminescent PS is that siloxene contains at least three oxygen atoms for every six silicon atoms. On freshly etched

luminescent PS , infra-red, and XPS (X-ray Photo-electron Spectroscopy) data indicate that very little, if any, oxygen is present [20].
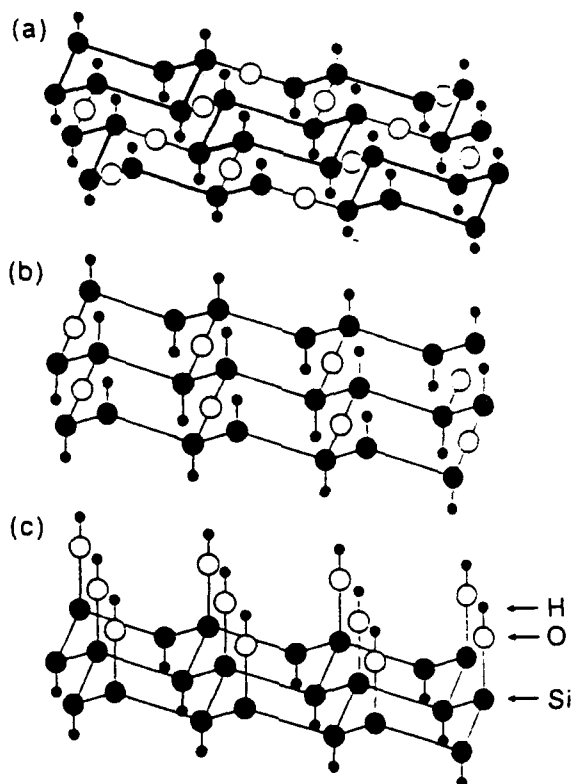
Fig.6.   Structural models for siloxene (a) Monolayers formed by hexagonal silicon rings interconnected by oxygen bridges. The fourth bond of silicon is terminated by hydrogen. (b) Monolayers formed by linear Si chains interconnected by oxygen, terminated by hydrogen. (c) Silicon monolayers with alternating OH and H bond terminators after Brandt [21].

Pure siloxene ($Si_6O_3H_6$) prepared according to Kautsky *et al.* [22] is a greenish white powder with a weak room temperature fluorescence in the green. The structure of this material consists of layers formed by hexagonal silicon rings separated from each other by oxygen bridges. The remaining silicon dangling bonds are terminated by hydrogen (Fig.6a). Alternative structures are also shown in Fig.6b, 6c. The structure units here are linear silicon chains interconnected by oxygen or pure silicon layers with alternating OH and H bond terminators. The second

preparation method which has been originally described by Wöhler [23] leads to a bright yellow substance with a strong yellow fluorescence. The substance is believed to be a mixture of the different structural features in figure 6. Wöhlers compound is denoted by $Si_6O_{3+n}H_{6-m}$. The increase of the oxygen content (n) and the decrease of the hydrogen content (m) correspond to an increasing 3-dimensional cross linking of the layered structures by oxygen bridges. The fluorescence bands emitted by siloxene can be tuned in a well controlled way over a large spectral range via chemical substitution of hydrogen by other monovalent ligands such as halogen's, OH or alcohol groups. Alternatively, tuning can also be achieved by annealing of siloxene in air. The particular optical properties of this compound are due to linear chains and/or sixfold rings of Si atoms isolated from each other by ordered insertion of oxygen atoms into a planar array of silicon atoms. While the electronic states in the assumed quantum wires of PS would be confined physically due to the geometrical quantum size of the small columnar silicon crystallites, the confinement in siloxene can be linked with the chemical composition.

3.3 Alternative models

In alternative explanations dramatic luminescence of PS results from a surface or bulk phase of amorphous silicon (a-Si), amorphous hydrogenated silicon (a-Si:H), or amorphous hydrogenated silicon oxide (a-SiO$_x$:H) produced in the etching process. Just as graphite and diamond are polymorphs of carbon with profoundly different electronic properties, the amorphous phase of silicon has quite distinct properties with respect to crystalline silicon. Amorphous hydrogenated silicon has a pseudo direct bandgap which varies continuously between 1.5 to 2.55 eV depending on hydrogen content (which is considerably larger than the indirect bandgap of crystalline silicon of 1.12 eV) [24]. The bandgap enlargement is caused by localisation of electron-hole pairs by disorder. A similar increase in optical bandgap is caused by alloying in a-SiO$_x$:H [25].

4 EXPERIMENTAL STUDIES

After the initial discovery by Canham [4] of visible light emission in silicon many experiments were started by the scientific community. Most of them try to unravel the origin of the light emission from PS. Photoluminescence (PL) spectroscopy is the most frequently used technique. Here the light emission from a material under photonic excitation is studied spectroscopically. Other powerful techniques applied include Raman scattering, infra-red absorption spectroscopy and electron/tunneling microscopy.

4.1 Photoluminescence

Photoluminescence spectroscopy is a simple method to investigate PS properties. Room-temperature PL spectra are easily obtained by excitation by He-Cd (442.0 nm, 2.81 eV) or Ar$^+$ (488.0 nm, 2.54 eV) radiation. Lifetime studies showed PL lifetimes around 50 µs at 300 K to 2.5 ms at 4.2 K [26,27]. Such a long luminescence lifetime rules out laser applications at high switching speeds.

The high PL efficiency of PS in comparison to bulk silicon (maximum efficiencies around 10% are reported) was ascribed to the low surface recombination rate owing to surface passivation of hydrogen which decreases non-radiative recombination drastically [28].

Strong support for the quantum confinement model came from two recently published experiments. In the first a fine structure was reported on top of the PL spectrum at low temperatures <77 K. The 4.2 K photoluminescence band consists of a set of lines spaced nearly evenly, with the energy interval equal to about 50 meV [29]. The fine structure lines appear to be on identical positions for different samples [30]. This fine structure can be accounted for if we assume that the PL originates from quantization in silicon wires. The PL spectrum is determined by the distribution of transverse size of the wires (and/or of their different parts). Such a distribution is discrete rather than continuous, because there is a minimum value of the size change which is equal to an interatomic distance in the crystal. Theoretical calculations of this effect using Eq. 2 are in good agreement with experiment.

In the second experiment amorphous silicon (a-Si) layers were grown on top of (100) crystalline silicon substrate's. Some of the a-Si layers received an additional annealing step between 550-1150°C before being etched in HF-HNO$_3$-based solutions (see section 2). While no visible PL was observed from unannealed and etched samples, visible PL was detected after annealing and etching [31]. The observation of visible PL after etching coincided with the observation of silicon

micro-crystallites in the annealed layer. The result suggest that an initial crystalline structure is important for fabricating luminescent porous silicon layers.

For Light Emitting PS there has been a severe problem with instability and degradation in the light emission. It was found that laser induced oxygen absorption is the major cause for the light emission degradation [32,33]. A sharp reduction in PL is also observed for annealing at temperatures >300°C, this coincides with desorption of hydrogen from the SiH_2 surface species [34-37].

Some PL experiments are at present not understood in terms of the quantum confinement model. One of them is the dependence of the peak PL energy at 300 K on excitation energy as depicted in Fig.7 as observed by Fuchs et al. [38]. They observed, however, the same functional dependence for siloxene. In another PL experiment a redshift in the PL peak energy was observed versus annealing temperature [19]. This redshift has similarities with the optical band-gap dependence on heating temperature as observed for a-Si:H [39].

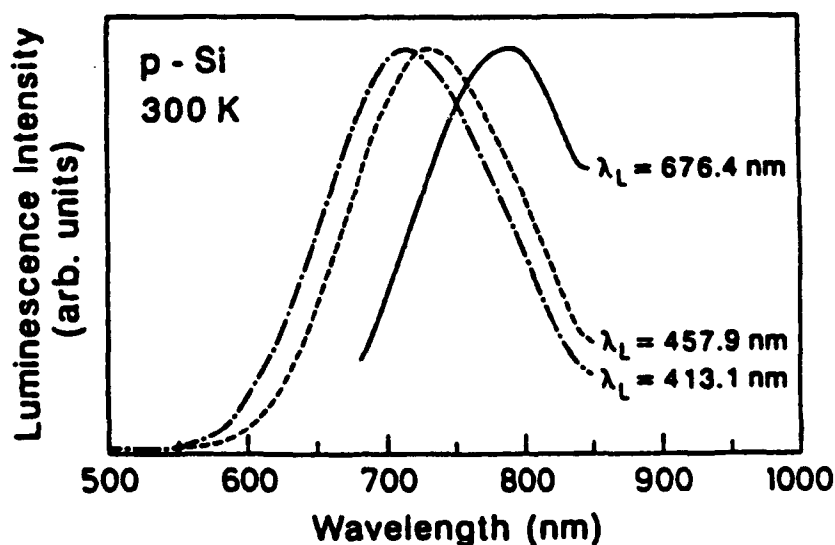
Fig.7.   Normalized luminescence spectra for porous silicon at 300 K showing the dependence of the luminescence peak position on the excitation wavelength, λ_L.

4.2   Raman scattering

Raman scattering is a non-destructive tool that is useful in the characterisation of semiconductors. Among other things it has been used to determine grain sizes in micro-crystalline materials. The

first-order Raman peak in c-Si is shifted by 520.5 cm^{-1}; it is symmetric and has a width of 3 cm^{-1} (FWHM). As the grain size in micro-crystalline silicon decreases below 200 Å, the Raman shift decreases, the width increases, and the peak becomes increasingly asymmetric, with an extended tail at low frequencies. The Raman spectrum of amorphous silicon peaks near 480 cm^{-1} and is usually weak in intensity and very broad. Macro-Raman studies on PS found shifts in the range 508.0 - 510.1 cm^{-1} [40]. The parameters of these spectra lie between those of micro-crystalline silicon and amorphous silicon, and can be accounted for in a theory by Campbell and Fauchet [41] if we assume that PS consists of sphere-like micro-crystalline material. Micro-Raman spectroscopy identified also amorphous silicon in PS regions emitting visible PL [42].

4.3 Other techniques

Microscopic studies using high-resolution transmission electron microscopy (TEM) reveal that porous silicon consists of silicon crystallites. The crystallites are approximately 3.5 nm in size and are randomly distributed throughout the PS region [43]. There appears to be no evidence for needle-like or column-like structures. On the contrary Gonchond *et al.* [44] identified in high resolution scanning electron microscopic (HRSEM) images pore structures in the 3 to 10 nm range, they ascribed the absence of individual pores in TEM images to the overlapping random morphology.

Fourier transform infra-red spectroscopic studies have shown that predominant silicon monohydride (SiH) termination results in weak PL. In contrast, it has been observed that the appearance of silicon dihydride (SiH$_2$) coincides with an increase in the PL intensity [35].

5   ELECTRO-LUMINESCENCE

Although optical stimulation of porous silicon is valuable for studies of material properties, the ability to produce luminescence electrically is a necessity for practical device applications. The first electro-luminescence (EL) reports were published in July 1991 by Halimaoui *et al.* [45]. They observed an unstable electro-luminescence during anodic oxidation in an electrolyte (aqueous solution of 1% HCl or KNO_3). The red-orange light emission is visible over the entire surface of the wafer even at day light. The EL stops when a continuous oxide layer is formed at the PS crystalline silicon interface.

Solid state electro-luminescent devices were also fabricated [46-49]. They were made by depositing an electrically conducting, transparent layer on top of the porous silicon. The Münich group [46] used a thin gold layer of 12 nm. This is thin enough to permit light to pass (transmission above 80%). On the back side of the wafer another contact layer of 300 nm gold was used. If a current over 5 mA at 200 V is passed through the film light emission is observed for dc currents of both polarities and ac currents. This is an unexpected result and has to be explained in the future. Light emission is only observed for n-type silicon. No degradation was observed after 45 minutes of operation.

Namavar and co-workers [47] made use of indium tin oxide (n-type semiconductor, ITO) as transparent conductor. In order to make a light-emitting diode (LED) structure p-type silicon was used as basis material for PS fabrication. Light emission emanating from the top surface was only observed under forward bias conditions and lasted at least 5 hours after which the experiment was stopped. Its operation is better understood than the previous described device. A forward bias applied to the base silicon allows holes to enter the porous silicon region. Electrons can then be injected into the PS's from the n-type ITO layer and electro-luminescence results from recombination between the injected electrons and the majority-carrier holes within the silicon nanostructure. In general the quantum efficiency of the devices is low (typically 10^{-4}%).

6 EXPERIMENTAL

6.1 Anodic oxidation

Both n- and p-type silicon wafers with low dopant concentrations were used for PS fabrication. The back-side of the silicon wafer was covered with 300 nm Al, deposited by e-beam evaporation, and served as electrical contact. Anodic oxidation was performed in ethanoic HF (49%), $HF:C_2H_5OH = 1:1$ at current densities in the range 50 - 200 mA/cm^2. The ethanol was added as wetting agent reducing inhomogeneous etching caused by sticking of hydrogen bubbles to the silicon surface. One electrode was attached to the top and back-side of the wafer. A Pt wire served as counter electrode. Beewax was used to protect the aluminium contact film on the silicon against HF when submersed in the electrolyte. The silicon samples were illuminated with a halogen lamp during etching in case n-type silicon substrate's were used (see section 2). The PL properties of thus produced PS could be checked with a hand-held mercury lamp as excitation source. All samples emitted red-orange light. The wafers appeared black at day light illumination when low anodisation current densities were used. The colour changed to brownish, yellowish at increased current densities. Samples did not receive any additional etching in HF-based solutions.

6.2 PL-spectrometer

To check the PL characteristics a PL spectrometer was assembled. We used a HeCd excitation source (442.0 nm, 14 mW). The laser beam width was enlarged with cylindrical lens systems resulting in power densities on the PS sample adjustable between 10 to 50 mW/cm^2. The PL from the PS sample was focussed on a 2mm entrance slit of a double prism monochromator. The light was detected using state of the art lock-in techniques using a silicon photodiode. Optimum S/N ratios were obtained for low modulation frequencies of a few Hertz. Two filters were placed in the light path from laser to monochromator. A laser interference filter (Centre: 441 nm, bandwidth 8 nm) was placed just in front of the laser and was crucial in eliminating pump laser light to enter the photodiode. A colour filter was placed right after the sample and was blocking scattered laser light.

6.3 ITO sputtering

Indium tin oxide (ITO) layers were deposited by sputtering. We used a commercial turbo-molecular pumped RF sputtering system of Alcatel. It allowed RF-diode or RF-magnetron

sputtering from 4 inch targets. A metallic indium-tin target (In:Sn = 9:1, by mass) was reactively sputtered with high purity oxygen (99.995%). Typical sputtering parameters are : RF-power 600 W, sputtergas pressure 2.10^{-3} mbar, base pressure 3.10^{-7} mbar, substrate target distance 50 mm. The sample was mounted on a copper plate which could be heated up to 450°C.

7   RESULTS AND DISCUSSION

A scanning electron microscopic image of a porous silicon surface produced from n-type silicon
is depicted in Fig.8. The pore structure is clearly demonstrated. The luminescence spectrum of
such a sample as recorded with our spectrometer is shown in Fig.9. It resembles the PL spectra
published in literature.

Fig.8   SEM micrographs of n-type porous silicon layer, top view (left) and side view (right)
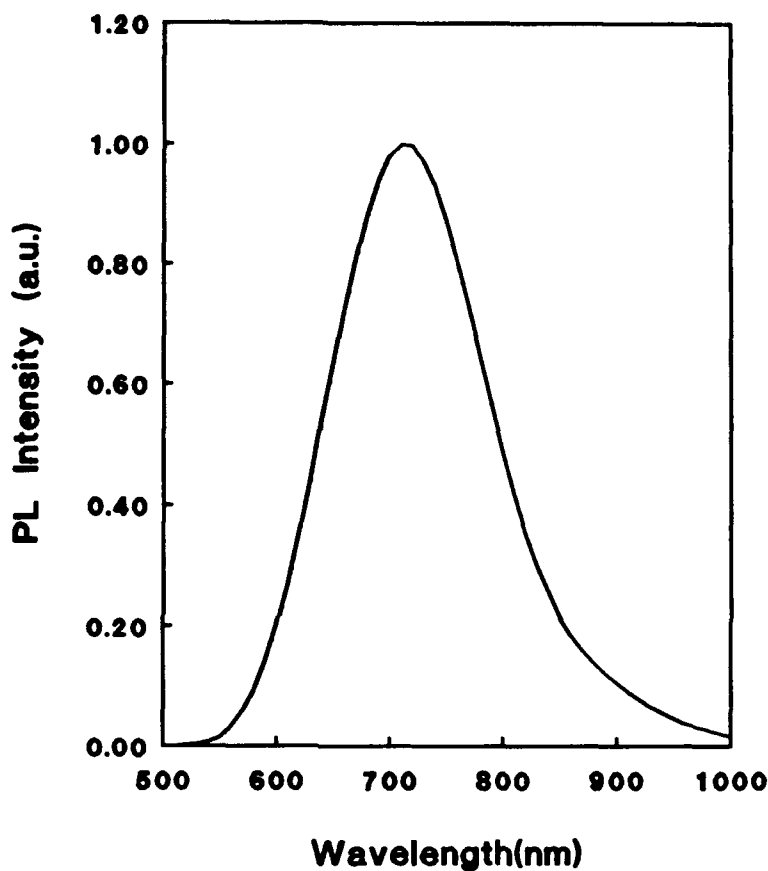
Fig.9   Typical room temperature photoluminescence spectrum of n-type porous silicon.

All recorded PL spectra had peak intensities in the range 670 - 740 nm. Anodisation current density and time hardly affected the peak position. When the PS samples were excited with light intensities in the range 10 - 50 mW/cm² under atmospheric conditions a luminescence degradation was observed. The degradation being more severe for higher light intensities (see Fig.10).
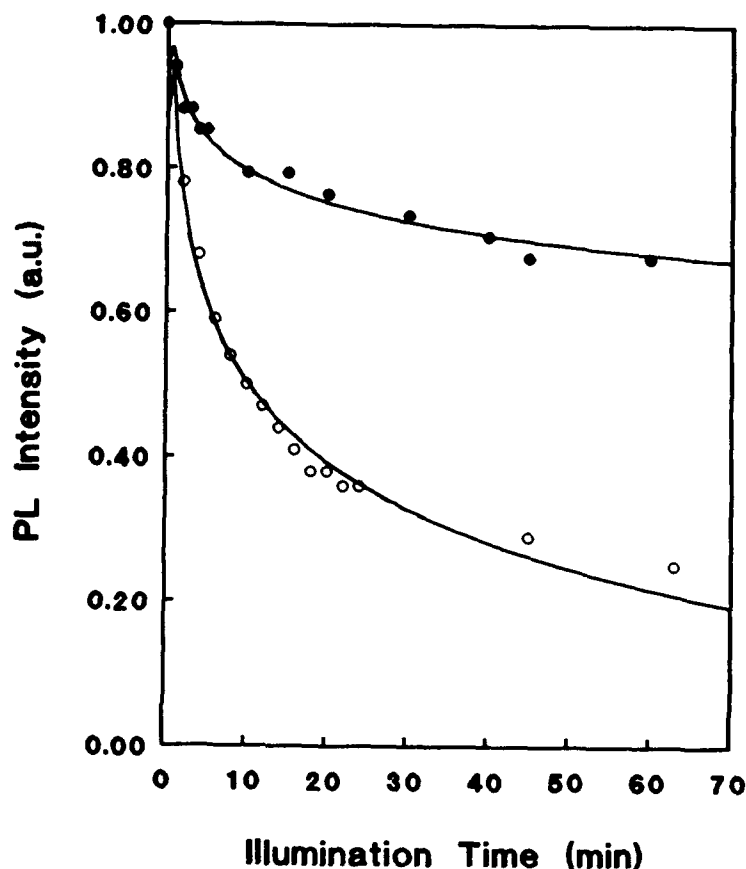
Fig.10   Photo luminescence degradation as function of illumination time. Light intensities: closed circles 20 mW/cm^2, open circles 50 mW/cm^2.

Xu *et al.* [50] noted that degradation only occurred in oxygen rich environments. Since PL degradation only occurred for a sample simultaneously exposed to oxygen and irradiation they concluded that it was caused by a photo-chemical reaction, probably an oxidation reaction. Several questions remained however: (1) Why would SiO$_x$ formation on the silicon surface quench the PL intensity, it is known e.g. that anodic oxidation does not destroy PL properties; (2) Why is illumination necessary, while it is well known that oxide formation occurs quite readily in the dark. We observed that partial recovery of the PL by room-temperature annealing is possible after degradation at low light intensities, which raises yet another question.

The electronic bands of semiconductors shift upon pressure. It changes not only the bandgap energy but also the relative position of the bands, and its curvature (effective masses). This property is nowadays heavily used in laserdiode fabrication. Bandgap tuning allows a broader range in laser wavelength, lower internal losses, lower threshold current density, etc. Chan *et al.* [51] removed a thin semiconductor film and re-attached it to a non-planar host substrate, which

contains raised ribs. Consequently there is a spatial modulation in the strain near the ribs, and this, in turn modulates the bandgap through the deformation potential. In the grafted film a GaAs/AlGaAs quantum well is used to probe the bandgap. Near the rib a red shift of 62 meV in the quantum well photo-luminescence is observed and attributed to the strain-induced change in bandgap.

To shed some light upon the PL origin in PS a strain-induced shift could bring important information since the strain dependence of the electron bands in mono-crystalline silicon is well documented. In our experiment we applied an uniaxial pressure to the porous silicon by bending the silicon substrate. The wafer was clamped on one side, while a screw was pressing on the opposite side at the back-side of the wafer. Several PL spectra were recorded for increased bending of the wafer. Until the breaking point no detectable change in the PL peak position was observed. One can conclude that either the PL of PS does not originate from confined carriers, or that the PS is not sufficiently stressed in the present experiment. One could easily imagine that the porous structure created by the anodic etching easily adjust to lateral stresses by reducing the empty space between the silicon columns. In a second attempt we made use of surface acoustic waves (SAW) which enabled us to induce transversal stresses in the PS. For this purpose a silicon wafer was sputtered with poly-crystalline ZnO, a highly piezo-electric material ideally suited for generation of SAW. The centre of the wafer was not covered with ZnO, it was left open for PS fabrication. On top of the ZnO 300 nm aluminium was deposited using e-beam evaporation. Via lithographic techniques and wet etching two transducers were formed in the aluminium, one on each side of the intended PS region. One served as transmitter, one as receiver. After PS fabrication the SAW device was tested. From the absence of any signal on the receiver we concluded that the SAW could not penetrate through the PS region and were strongly damped. No attempt was therefore made to observe the influence of a SAW on the PL spectrum of PS. In a future experiment one could try to stress the PS transversal by applying pressure through a quartz rod, which allows excitation light to enter and PL light to leave the stresses PS region.

In the mean time a paper was published by Zhoe et al. [52] who measured PL of PS under hydrostatic pressure up to 37 kbar using a diamond anvil cell. It is well known that bulk crystalline silicon has a pressure coefficient of about -1.4 meV/kbar for the indirect gap at 1.1 eV [53] and 5.2 meV/kbar for the direct gap at 3.4 eV [54] whereas amorphous hydrogenated silicon (a-Si:H) has a pressure coefficient of about -2 meV/kbar [55]. The pressure coefficients for siloxene are thusfar unknown. Zhoe et al. observed in their experiments a large blue shift of the PL. The blue shift depended on sample preparation, and is in the wrong direction to be consistent with PL from either a-Si:H or the indirect bandgap of bulk c-Si. In contrast to these reports Sood

et al. [56] observe giant red shifts in similar experiments. The red shift is much bigger than expected for a-Si:H or bulk c-Si.

The measurements thus far are not conclusive. There is the need for more thorough experiments. Also the pressure coefficients of siloxene have to be measured. Sample preparation and sample history might play an important role in these experiments.

Electro-luminescence (EL) is most readily observed using anodic oxidation techniques as first described by Halimaoui [45]. We immersed a PS sample just produced in a 1% HCl solution. When a current was passed through the wafer visible light emission from the PS surface was observed. If the anodisation current was switched off, the light ceased. The light also extinguished after some anodisation time, coinciding with a rise in anodisation potential at constant current conditions. Due to a single point contact no homogenous oxidation and electro-luminescence was observed.

In order to produce stable electro-luminescence a heterostructure was made of p-Si and n-type indium tin oxide (ITO). The ITO contact layer should be optimized for transparency and conductivity. At first glass plates were sputtered (RF-diode) with ITO layers using the sputtering equipment described in section 6.3. Substrate temperatures varied from room temperature to 400°C (100°C intervals). All films had equal transparency up to 80% @ 632.8 nm, except for a sample sputtered at room temperature which was not transparent at all. Electrical conductivity increased for higher substrate temperatures. Since it is known that PS is destroyed for annealing temperatures above 300°C we sputtered ITO on some PS samples at 100 and 200°C. After the sputter deposition PL was no longer visible. Various experiments pointed out that the combination of oxygen ambient and heating up to 100 - 200°C did not degrade the PL. The PL degradation is caused by the RF-diode sputtering process. It is known that the growing film in RF-diode sputtering processes is bombarded by high-energetic particles [57]. This bombardment can be reduced considerably using the magnetron sputtering technique. Preliminary experiments showed that PL remained after magnetron deposition of ITO on top of PS. Unfortunately the conducting properties of thus sputtered ITO layers was extremely low. A working LED structure was therefore not obtained in the current project. Optimization of ITO deposition could not be accomplished fully, but is essential for production of a heterostructure LED device.

8 CONCLUSIONS

The fabrication of light emitting porous silicon is successfully demonstrated in the present research project. The production of homogeneous PS surfaces, however, requires an alternative anodisation set-up than the one employed in the current project. The PL spectrum of PS layers was measured with a room temperature PL-spectrometer using a HeCd laser as excitation source. Electro-luminescence could only temporarily be observed during anodic oxidation. LED diode structures using p-type silicon and indium tin oxide could not be demonstrated due to insufficient optimization of ITO layers.

No decisive experimental evidence is available at present or could be gathered from our limited stress experiments which identify the origin of the PL of porous silicon. The micro-second decay time of the PS luminescence rules out its application in fast switching laser application (telecommunications, optical computing), unless external modulators are used. This micro-second decay is much larger than the nanosecond decay of the usual direct bandgap semiconductors like GaAs, however it compares favourably with the decay of nitrogen doped GaP materials which are the materials of choice for visible light-emitting diodes in todays market. Combined with the mature silicon integrated circuit technology the PS material has the potential to compete in todays visible LED market. Two serious and important problems have to be solved in advance however. (1) The efficiency of electro-luminescence devices should be increased by a few orders of magnitude using practical carrier injection approaches. (2) The porous silicon degradation should be under control. The problem here is probably surface effects. The internal surface area of microporous silicon is of the order of 600 m^2/cm^3. There is a saying in the silicon community that the bulk of the silicon crystal was created by God, while the surface was made by the devil. It is obvious with whom one is dealing in the case of porous silicon. Because of the anticipated problems we do not foresee an immediate introduction of porous silicon based devices.

Porous silicon will attract a lot of scientific attention in the immediate future due to the extreme importance of visible light emission in silicon for the semiconductor industry. Because of its potential implications for our integrated optical devices (IOD) group a close watch on the future international research effort is crucial.
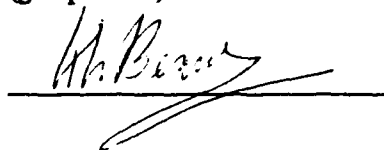
9   REFERENCES

[1]   W.J. Miniscalo, IEEE J. Lightwave Technol. 9, 234 (1991).

[2]   H.B. Dietrich, P.B. Klein, B.J. Mrstik, and P.C. Ingram, SPIE 530, 195 (1985).

[3]   L.T. Canham, K.G. Barraclough, and D.J. Robbins, Appl. Phys. Lett. 51, 1509 (1987).

[4]   L.T. Canham, Appl. Phys. Lett. 57, 1046 (1990).

[5]   R.W. Fathauer, T. George, A. Ksendzov, and R.P. Vasquez, Appl. Phys. Lett. 60, 995
        (1992).

[6]   R.L. Smith, and S.D. Collins, J. Appl. Phys. 71, R1 (1992).

[7]   C. Levy-Clement, A. Lagoubi, R. Tenne, and M. Neumann-Spallart, Electrochimica
        Acta 37, 877 (1992).

[8]   V. Lehmann, and U. Gösele, Appl. Phys. Lett. 58, 856 (1991).

[9]   L.T. Canham, M.R. Houlton, W.Y. Leong, C. Pickering, and J.M. Keen, J. Appl. Phys.
        70, 422 (1991).

[10]   M.I.J. Beale, J.D. Benjamin, M.J. Uren, N.G. Chew, and A.G. Cullis, J. Cryst. Growth
        73, 622 (1985).

[11]   C. Pickering, M.I.J. Beale, D.J. Robbins, P.J. Pearson, and R. Greef, J. Phys. C 17,
        6535 (1984).

[12]   M.I.J. Beale, I.D. Benjamin, M.J. Uren, N.G. Chew, and A.G. Cullis, Appl. Phys. Lett.
        46, 86 (1985).

[13]   R.L. Smith, S.-F. Chuang, and S.D. Collins, J. Electron. Mater. 17, 533 (1988).

[14]   S.-F. Chuang, S.D. Collins, and R.L. Smith, Appl. Phys. Lett. 55, 675 (1989).

[15]   F. Phillip, K. Urban, and M. Wilkens, Ultramicroscopy 13, 379 (1984).

[16]   L. Brus, IEEE J. Quantum Electron. 22, 1909 (1986).

[17]   H. Takagi, H. Ogawa, Y. Yamazaki, A. Ishizaki, and T. Nakagire, Appl. Phys. Lett.
        56, 2379 (1990).

[18]   M. Voos, Ph. Uzan, C. Delalande, and G. Bastard, Appl. Phys. Lett. 61, 1213 (1992).

[19]   M. Stutzmann, J. Weber, M.S. Brandt, H.D. Fuchs, M. Rosenbauer, P. Deak,
        A. Höpner, and A. Breischwerdt, Adv. Solid State Phys. 32, 179 (1992).

[20]   J.L. Heinrich, C.L. Curtis, G.M. Credo, K.L. Kavanagh, and M.J. Sailor, Science 255,
        66 (1992).

[21]   M.S. Brandt, M.D. Fuchs, M. Stutzmann, J. Weber, M. Cardona, Solid State Commun.
        81, 307 (1992).

[22]   H. Kautsky, and H. Zocher, Z. Phys. 9, 267 (1992).

[23]   F. Wöhler, Lieb. Ann. 127, 275 (1863).

[24]   D.J. Wolford, B.A. Scott, J.A. Reimer, and J.A. Bradley, Physica 117B & 118B, 920
         (1983).

[25]   R. Carius, R. Fisher, E. Holzenkämpfer, and J. Stuke, J. Appl. Phys. 52, 4241 (1981).

[26]   G.W. 't Hooft, Y.A.R.R. Kessener, G.L.J.A. Rikken, and A.H.J. Venhuizen, Appl.
         Phys. Lett. 61, 2344 (1992).

[27]   T.P. Pearsall, J.C. Adams, J.E. Wu, B.Z. Nosho, C. Aw, and J.C. Patton, J. Appl. Phys.
         71, 4470 (1992).

[28]   E. Yablonovitch, D.L. Allara, C.C. Chang, T. Gmitter, and T.B. Bright, Phys. Rev.
         Lett. 57,   249 (1986).

[29]   N.S. Averkiev, V.M. Asnin, I.I. Markov, A. Yu. Silov, V.I. Stepanov, A.B. Churilov,
         and N.E. Mokrousov, JETP lett. 55, 657 (1992).

[30]   G.L.J.A. Rikken, private communications.

[31]   K.H. Jung, S. Shih, D.L. Kwong, C.C. Cho, B.E. Gnade, Appl. Phys. Lett. 61, 2467
         (1992).

[32]   X.L. Zheng, H.C. Chen, and W. Wang, J. Appl. Phys. 72, 3841 (1992).

[33]   M.A. Tischler, R.T. Collins, J.H. Stathis, and J.C. Tsang, Appl. Phys. Lett. 60, 639
         (1992).

[34]   C. Tsai, K.-H. Li, J. Saranthy, S. Shih, J.C. Campbell, B.K. Hance, and J.M. White,
         Appl. Phys. Lett. 59, 2814 (1991).

[35]   C. Tsai, K.-H. Li, D.S. Kinosky, R.-Z. Qian, T.-C. Hsu, J.T. Irby, S.K. Banerjee,
         A.F. Tasch, J.C. Campbell, B.K. Hance, and J.M. White, Appl. Phys. Lett. 60, 1700
         (1992).

[36]   N. Ookubo, H. Ono, Y.Ochiai, Y.Mochizuki, and S. Matsui, Appl. Phys. Lett. 61, 940
         (1992).

[37]   M.B. Robinson, A.C. Dillon, D.R. Haynes, and S.M. George, Appl. Phys. Lett. 61,
         1414 (1992).

[38]   H.D. Fuchs, M. Stutzmann, M.S. Brandt, M. Rosenbauer, J. Weber, and M. Cardona,
         Phys. Scripta T45, 309 (1992).

[39]   S. Yamasahi, N. Hata, T. Yoshida, H. Oheda, A. Matsuda, H. Okushi, and K. Tanaka,
         J. Phys. C 42, 297 (1981).

[40]   Z. Sui, P.P. Leong, I.P. Herman, G.S. Higashi, and H. Temkin, Appl. Phys. Lett. 60,
         2086 (1992).

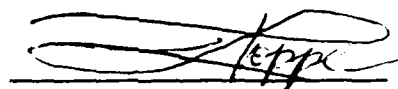[41]   I.H. Campbell, and P.M. Fauchet, Solid State Commun. 58, 739 (1986).

[42]   J.M. Perez, J. Villalobos, P. McNeill, J. Prasad, R. Cheek, J. Kelber, J.P. Estrera, P.D. Stevens, and R. Glosser, Appl. Phys. Lett. 61, 563 (1992).

[43]   M.W. Cole, J.F. Harvey, R.A. Lux, D.W. Eckart, and R. Tsu, Appl. Phys. Lett. 60, 2800 (1992).

[44]   J.P. Gonchond, A. Halimaoui, K. Ogura, Inst. Phys. Conf. Ser. 117, 235 (1991).

[45]   A. Halimaoui, C. Oules, G. Bomchil, A. Bsiesy, F. Gaspard, R. Herino, M. Ligeon, and F. Muller, Appl. Phys. Lett. 59, 304 (1991).

[46]   A. Richter, P. Steiner, F. Kozlowski, W. Lang, IEEE Electron. Device Lett. 12, 691 (1991).

[47]   F. Namavar, H.P. Maruska, and N.M. Kalkhoran, Appl. Phys. Lett. 60, 2514 (1992).

[48]   H.P. Maruska, F. Namavar, and N.M. Kalkhoran, Appl. Phys. Lett. 61, 1338 (1992).

[49]   N. Koshida, and H. Koyama, Appl. Phys. Lett. 60, 347 (1992).

[50]   Z.Y. Xu, M. Gal, M. Gross, Appl. Phys. Lett. 60, 1375 (1992).

[51]   W.K. Chan, T.S. Ravi, K. Kash, J. Christen, T.J. Gmitter, L.T. Florez, and J.P. Harbison, Appl. Phys. Lett. 61, 1319 (1992).

[52]   W. Zhou, H. Chen, J.F. Harvey, R.A. Lux, M. Dutta, F.Lu, C.H. Perry, R. Tsu, N.M. Kalkhoran, and F. Namavar, Appl. Phys. Lett. 61, 1435 (1992).

[53]   B. Weber, C.K. Kim, M. Cardona, and S. Rodriguez, Solid State Commun. 17, 1021 (1975).

[54]   R. Zallen, and W. Paul, Phys. Rev. 155, 703 (1967).

[55]   B.A. Weinstein, Phys. Rev. B 23, 787 (1981).

[56]   A.K. Sood, K. Jayaram, D. Victor, and S. Muthu, J. Appl. Phys. 72, 4963 (1992).

[57]   D.J. Kester, and R. Messier, J. Vac. Sci. Technol. A 4, 496 (1986).

A.N. de Jong
(group leader)

H.H.P.Th. Bekman
(author)

K.W. Benoist
(author)

J.L. Joppe
(author)

H.J. van Weerden
(author)

REPORT DOCUMENTATION PAGE   (MOD-NL)

1. DEFENSE REPORT NUMBER (MOD-NL)	2. RECIPIENT'S ACCESSION NUMBER	3. PERFORMING ORGANIZATION REPORT NUMBER
TD93-0302		FEL-92-B047

4. PROJECT/TASK/WORK UNIT NO.	5. CONTRACT NUMBER	6. REPORT DATE
22539	-	MAY 1993

7. NUMBER OF PAGES	8. NUMBER OF REFERENCES	9. TYPE OF REPORT AND DATES COVERED
30 (EXCL. RDP & DISTR.LIST)	57	FINAL REPORT

10. TITLE AND SUBTITLE
LIGHT EMITTING POROUS SILICON

11. AUTHOR(S)
H.H.P.TH. BEKMAN, K.W. BENOIST, J.L. JOPPE, H.J. VAN WEERDEN

12. PERFORMING ORGANIZATION NAME(S) AND ADDRESS(ES)
TNO PHYSICS AND ELECTRONICS LABORATORY, P.O. BOX 96864, 2509 JG THE HAGUE
OUDE WAALSDORPERWEG 63, THE HAGUE, THE NETHERLANDS

13. SPONSORING/MONITORING AGENCY NAME(S)
MOD-NL

14. SUPPLEMENTARY NOTES
THE CLASSIFICATION DESIGNATION ONGERUBRICEERD IS EQUIVALENT TO UNCLASSIFIED.

15. ABSTRACT (MAXIMUM 200 WORDS, 1044 POSITIONS)
AFTER A REVIEW OF THE BASIC PROPERTIES OF POROUS SILICON WE DESCRIBE THE FABRICATION METHOD WE EMPLOYED TO PRODUCE VISIBLE LIGHT EMISSION FROM SILICON. THE PHOTO-LUMINESCENCE SPECTRA WERE RECORDED USING A ROOM-TEMPERATURE SPECTROMETER. INITIAL ATTEMPTS PRODUCING ELECTRICALLY STIMULATED LIGHT EMISSION ARE DESCRIBED. TWO PRESSURE EXPERIMENTS WERE CARRIED OUT TO UNRAVEL THE ORIGIN OF LIGHT EMISSION IN POROUS SILICON.

16. DESCRIPTORS	IDENTIFIERS
LUMINESCENCE, SOLID STATE	POROUS SILICON
INTEGRATED OPTICS	
LIGHT EMITTING DIODES (LED)	
CHEMICAL ETCHING	
SILICON	

17a. SECURITY CLASSIFICATION (OF REPORT)	17b. SECURITY CLASSIFICATION (OF PAGE)	17c. SECURITY CLASSIFICATION (OF ABSTRACT)
ONGERUBRICEERD	ONGERUBRICEERD	ONGERUBRICEERD

18. DISTRIBUTION/AVAILABILITY STATEMENT	17d. SECURITY CLASSIFICATION (OF TITLES)
UNLIMITED	ONGERUBRICEERD

Distributielijst

1.	Hoofddirecteur TNO-Defensieonderzoek
2.	Directeur Wetenschappelijk Onderzoek en Ontwikkeling
3.	HWO-KL
4.	HWO-KLu
5.	HWO-KM
6.	
t/m	Hoofd TDCK
8.	
9.	KIM, t.a.v. Dr.ir. J.H. Hendriks
10.	Directie FEL-TNO, t.a.v. Dr. J.W. Maas
11.	Directie FEL-TNO, t.a.v. Ir. J. Vogel, daarna reserve
12.	Archief FEL-TNO, in bruikleen aan Ir. J. Bennema
13.	Archief FEL-TNO, in bruikleen aan Drs. C.W. Lamberts
14.	Archief FEL-TNO, in bruikleen aan Ir. A.J. de Jong
15.	Archief FEL-TNO, in bruikleen aan Drs. R.J.L. Lerou
16.	Archief FEL-TNO, in bruikleen aan Dr. H.H.P.Th. Bekman
17.	Archief FEL-TNO, in bruikleen aan Drs. K.W. Benoist
18.	Archief FEL-TNO, in bruikleen aan Drs. J.L. Joppe
19.	Archief FEL-TNO, in bruikleen aan J.A.G. van Bezooijen
20.	Archief FEL-TNO, in bruikleen aan H.J. Eradus
21.	Archief FEL-TNO, in bruikleen aan Ir. A.J.T. de Krijger
22.	Documentatie FEL-TNO
23.	
t/m	Reserves
25.	